

Numerical Approach for the Mechanical Behavior of Fully Grouted Anchorage System Subjected to Pullout Test

Dunhua Lu

Department of Resources and Environmental Engineering, Henan Institute of Engineering, Zhengzhou, 451191, Henan, China

e-mail: ludunhua2009@126.com

ABSTRACT

Anchorage system has been applied in many engineering projects, such as slope strengthening, tunnel supporting and mining. Different mechanical models of anchorage system have been built. But the numerical simulation for the anchorage system pullout tests has seldom been done. In this paper, a numerical approach able to predict the mechanical behaviour of anchor subjected to pull-out tests is proposed. The mechanism of the anchor system is given, input parameters of such approach are: anchor geometry size, anchor's Young modulus, anchor's Poisson's ratio, and the constitutive law of the anchor-grout-soil interface with their parameters: friction angle, cohesion, shear stiffness and normal stiffness. Numerical solutions for the following aspects are done: distribution of anchor axial stress, response of the soil, the effect of the surrounding stress to the limit anchoring force, and the effect of the anchor length to the limit anchoring force.

KEYWORDS: Anchorage system; anchor; pullout test; numerical; simulation; interaction, mechanism.

INTRODUCTION

Anchorage system has been applied in many engineering projects^[1,2], such as slope strengthening, tunnel supporting and mining. The strengthening mechanism of anchorage system has been studied by many researchers in the past several decades^[3-6]. Different mechanical models of anchorage system have been built. For instance, Yang et al.^[3] and Wu et al.^[4] suggested a pull-out model of anchorage system with two different boundaries using a shear-lag model. Delhomme and Debicki^[5] studied the behavior of long and smooth anchor rod with enlarged head considering the visco-elastic behavior of epoxy described by the creep laws. Milligan and Tei examined the fundamental interaction mechanisms between anchor and soil during pullout^[6]. Anchorage systems have a high ratio of the circumference to the cross-sectional area, and therefore they rely essentially on frictional resistance for the load transfer, the pullout test is the main method to obtain the reinforcement mechanical parameters^[7-9], some scholars studied these

parameters by the insitu-tests^[10-12], which will cost great and cause some errors due to the complicated interaction between anchor and soil. So it is necessary to find some other methods to solve this problem. Fortunately, in recent years, rapid advances in computer technology and sustained development have pushed the numerical analysis methods like the fast lagrangian analysis of continua three dimensions (FLAC3D) to the forefront of geotechnical practice^[12-15]. In the present paper, a numerical approach able to predict the mechanical behaviour of anchor subjected to pull-out tests is proposed. The mechanism of the anchor system is given. Numerical solutions for the following aspects are done: distribution of anchor axial stress, response of the soil, the effect of the surrounding stress to the limit anchoring force, and the effect of the anchor length to the limit anchoring force.

MECHANISM OF ANCHOR REINFORCEMENT

The cohesive effect during anchor and foundation is the main factor influencing the reinforcement degree, which is related to not only the construction method, but also the property of soil mass. The interaction mechanism between soil and anchor is very complicated. According to the simplification point of view, when anchor takes effect in the soil, it mainly supports the tensile stress. The double-spring anchor element^[16] is adopted, shown in Fig.1.

The relative displacement among anchor, grout and soil mass is calculated by the relative displacement of anchor-grout system and grout-soil system. When the relative slippage takes place in each system, the shear characteristic of grout can be described by a series of anchor parameters and grout parameters. During the numerical calculation, anchor is divided into many small parts, and its deformation and stress state are obtained by integrating the corresponding response of these small parts.

The axial force of anchor element F_t^a can be obtained by its axial displacement u_{bt} ,

$$F_t^a = K_t^a u_{bt} \quad (1)$$

where, $u_{bt} = u_i^k n_i = (u_x^{[2]} - u_x^{[1]})n_1 + (u_y^{[2]} - u_y^{[1]})n_2 + (u_z^{[2]} - u_z^{[1]})n_3$; $u_i^{[m]}$ is the displacement of node m in the i direction; n_i is the direction cosine of anchor axis.

The shear behavior of the anchor-soil interface is cohesive and frictional in nature. The system is represented numerically as a spring-slider system located at the nodal points along the anchor axis. Shear behavior of the system, is described by the anchor/grout interface and the grout/soil interface, shown in Fig 2. The grout annulus is assumed to behave as an elastic-perfectly plastic solid. As a result of relative shear displacement, between the tendon surface and the borehole surface, the shear force of anchor is,

$$\frac{F_s^a}{L} = K_s^a u_{bs} \quad (2)$$

where F_s^a is the shear stress of grout annulus; u_{bs} is the relative displacement between of anchor-soil interface; L is the effective reinforcement length; K_s^a is the shear stiffness of grout.

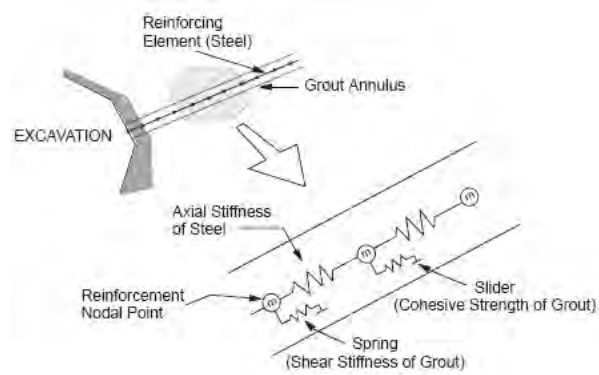


Figure 1: Anchor element

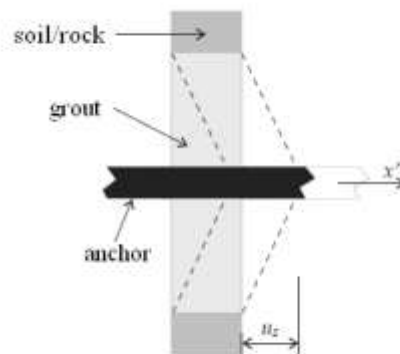


Figure 2: The deformation model of anchor

As a result of relative shear displacement for grout element u^t , the shear force of grout can be obtained,

$$F^t = k_g u^t \quad (3)$$

After deduction, the shear stress of grout-soil interface can be obtained for per length,

$$\tau_g = \frac{G \cdot \Delta u}{(D/2+t) \ln(1+2t/D)} \quad (4)$$

where Δu is the relative displacement of grout-soil interface; G is the shear modulus of grout; t is the thickness of grout; D is the diameter of anchor.

NUMERICAL CALCULATION MODEL

The commercial program FLAC3D is used to establish the numerical calculation model for simulating pullout test of anchor, shown in Fig.3, the size of the model is 4 m length, 4 m width and 7 m height. The soil is described by the elastic model for the purpose of mainly focusing on the interface reaction between anchor and soil. During the numerical test, the anchor is loaded with the velocity of 1.0×10^{-3} mm/step at the anchor head tip. Parameters for the soil is, 20.0 MPa elastic modulus, 0.3 Poisson's ratio; parameters of the anchor is 5.0 m length, 100.0 GPa elastic modulus, 0.25 Poisson's ratio, 706.5 mm^2 sectional area, 314 mm perimeter, $1.0 \times 10^9 \text{ N/m}^2$ stiffness of interface between anchor and soil, 15.0 kPa cohesion of interface, 25° friction angle of interface. The calculation convergence criterion is the unbalance force ratio criterion^[16], in which the maximum unbalance force is divided by the average nodal force. The calculation system is considered to be in the balance degree, when the unbalance force ratio is lower than 10^{-5} .

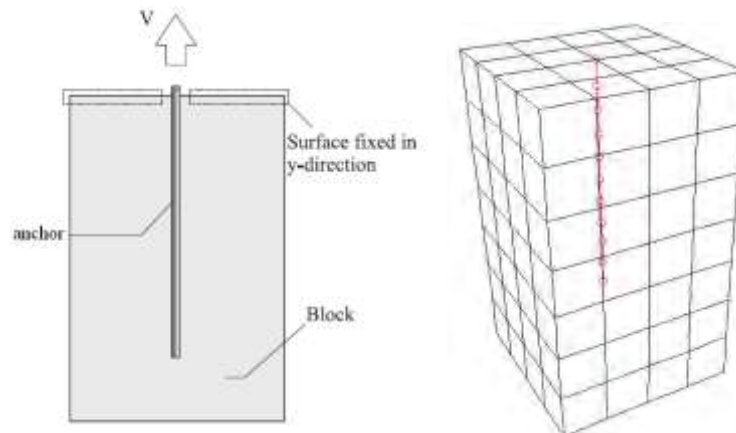


Figure 3: Calculation model for anchor subjected to pullout test

RESULTS AND DISCUSSION

Distribution of anchor axial stress

The axial stress of anchor during pullout procedure, and the variation for the axial force of anchor are shown in Fig.4 and Fig.5, each line in the figure indicates the variation of the axial force at different parts of anchor. From the figure, it can be seen that the axial stress distributed along the anchor shaft, the axial stress exhibits the maximum value at the anchor head tip, and decreases along the anchor shaft, which has the same trend discipline of the insitu-test^[10-12]. At the initial phase of pullout test, with the increase of the displacement of the anchor head, the anchoring force increases gradually. When the displacement of anchor head reaches some magnitude, the axial stress at each part of anchor reach their maximum value. At the initial phase of pullout test, the slipping failure only occurs at the anchor head, while with the loading going on, the failure propagates quickly, then lead to the whole failure of the anchor. At the final phase of pullout test, the anchoring forces reach its maximum value and remain unchanged, which indicates the whole failure of the anchor.

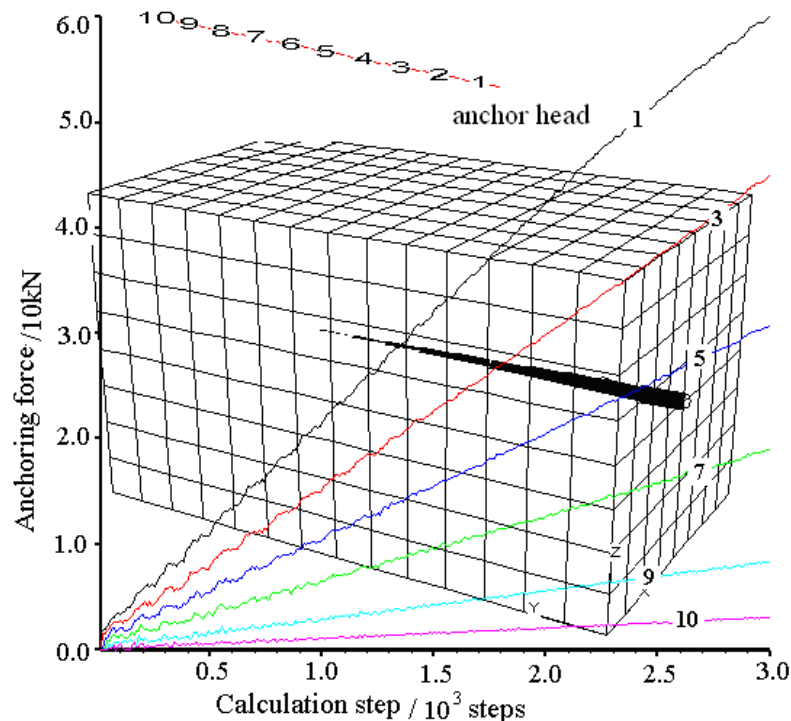


Figure 4: Axial stress of anchor at the initial phase of pullout

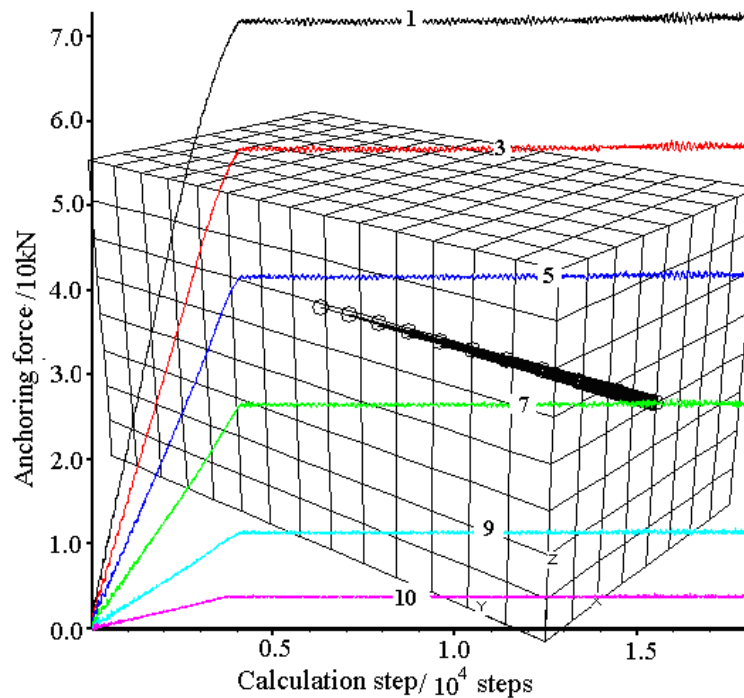
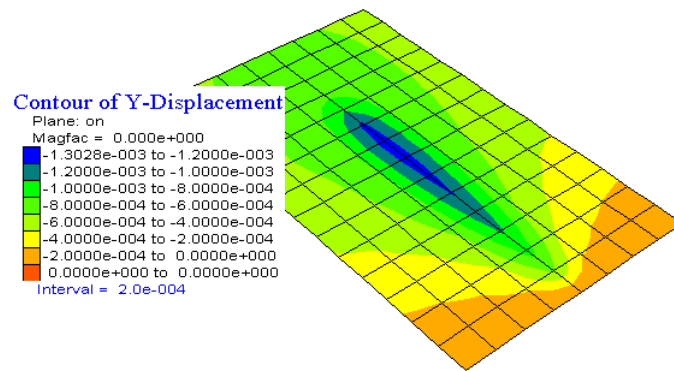


Figure 5: Axial stress of anchor at the final phase of pullout

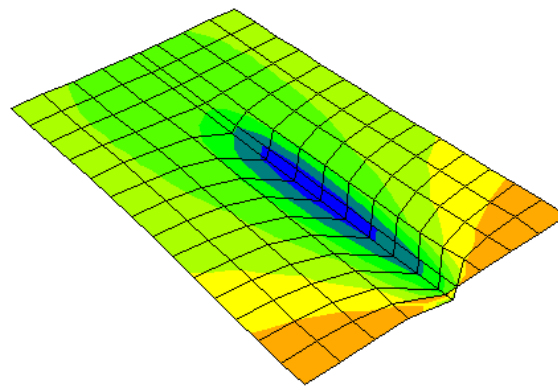
Response of the soil

Fig.6 shows the displacement response of soil along the anchor shaft direction during the pullout test. From the figure, it can be seen that, the soil mass tends to be pulled out by anchor with the friction force of interface between anchor and soil mass, the maximum value of the soil displacement is 1.3 mm, which is far smaller than that of anchor head; the maximum value of displacement of soil is at the anchor tail, and shown in the circular form to expand to the outside gradually. And due to the compressive effect by anchor, the surrounding soil mass tends to move to sideward.

The stress contour of the soil along the anchor shaft direction is shown in Fig.7. From the figure, it can be seen that, the pre-stressed anchor forms two stress concentrated areas: one is at the anchor head, which is the surface compressive area, another is at the anchor tail tip. The stress concentrated areas are induced by the compressive effect of the anchor to the soil. The influencing area by the compressive effect is about 2.0 ~3.0 m around, in which the compressive stress and compressive deformation show the maximum magnitude at the anchor head. And the concentrated area at the anchor tail is caused by that the compressive stress and tensile stress meet together.



(a) soil displacement contour along anchor shaft



(b) Soil deformation trend along anchor shaft

Figure 6: Displacement of soil along anchor shaft

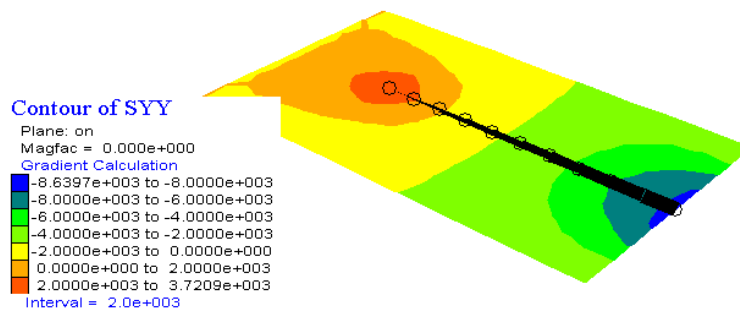


Figure 7: Soil stress along anchor shaft

The effect of the surrounding stress to the limit anchoring force

Fig.8 shows the relationship between anchor head displacement S and the tensile load Q . From the figure, it can be seen that, with the increase of tensile displacement, the anchoring force exerted by the anchor increase as well; and if the surrounding stress of the soil is small, the relationship between the load and displacement shows the nonlinear characteristic, while with the increase of the surrounding stress of soil, the relationship between the load and displacement shows the linear characteristic.

With the increase of surrounding stress σ_m of soil, the limit anchoring force of anchor increases as well, as shown in Fig. 9. Relationship between failure load of anchor and surrounding stress can be fitted by exponential equation with high coefficient. The increase of the surrounding stress σ_m can increase the friction between soil and anchor, but there exist a limit value of σ_m , if the surrounding stress surpass the limit value of σ_m , the anchoring force of anchor can no longer be increased by only increasing the surrounding stress of soil. In the model studied, the limit anchoring force is 266 kN.

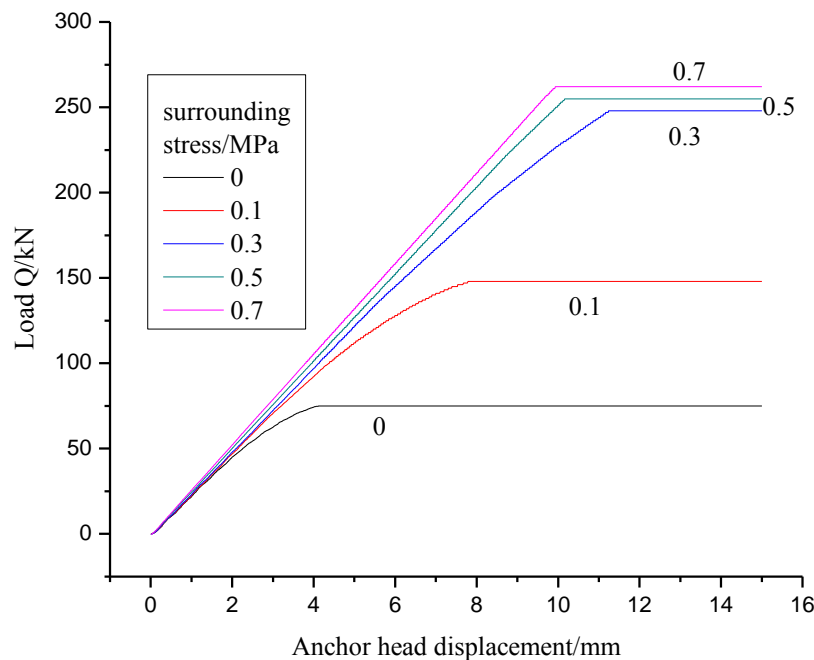


Figure 8: Loading-displacement of anchor head

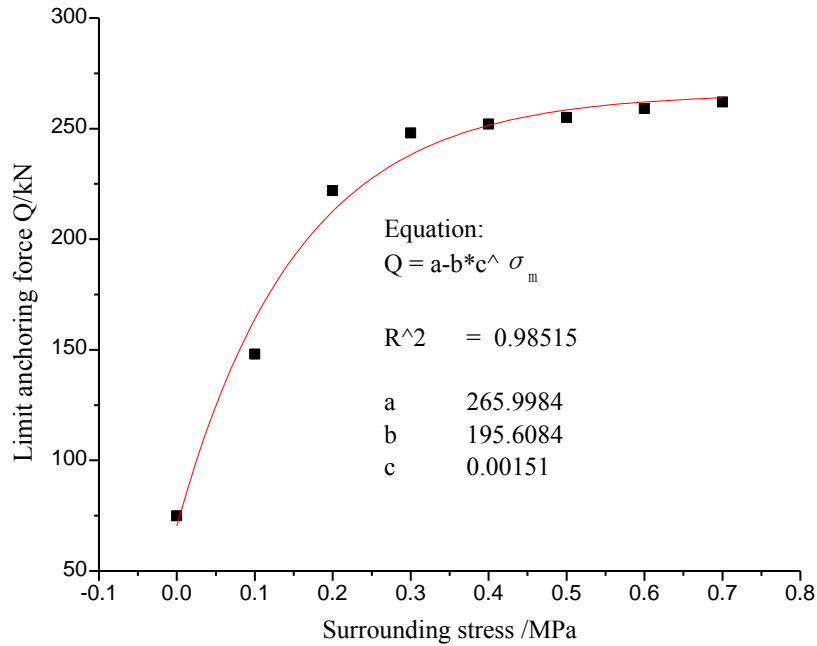


Figure 9: Relationship between limit anchor force and surrounding stress of anchor

Effect of the anchor length to the limit anchoring force

Fig.10 shows the relationship between limit anchoring force of anchor and its length. From the figure, it can be seen that, the relationship between limit anchoring force of anchor and its length shows in the linear form. If the linear fitting is applied to their relationship, the fitting coefficient is 0.99991, which indicates good fitting result. Then increasing the anchor length is an effective way to increase the anchoring force of anchor reinforcement system. The relationship of anchor with different anchor length and the anchoring force is shown in Fig.11. From the figure, we can see that, with the increase of anchor length, the anchor limit anchoring force increase gradually, and the relationship curves are all in the nonlinear form before they reach the peak value.

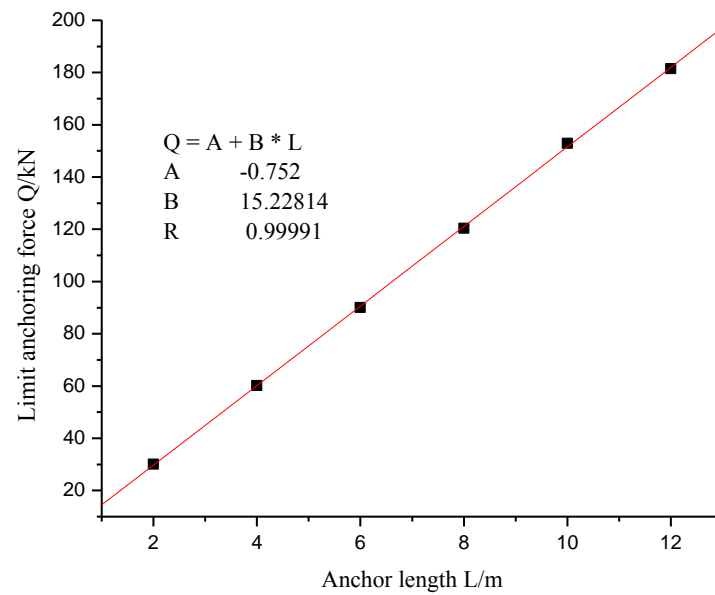


Figure 10: Relationship between limit anchor force of anchor and its length

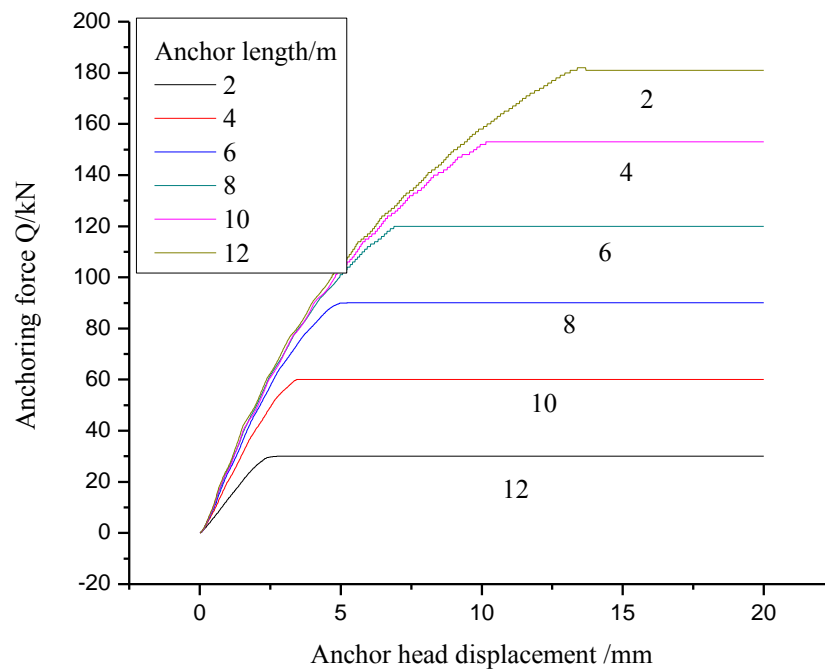


Figure 11: Relationship between anchor force and displacement of anchor head with different length

The axial stress propagates procedure

Suppose the time needed for excavation is t , then the axial stress propagation is shown in Fig.12 during the anchoring procedure. From the figure, it can be seen that, along the anchor shaft, the anchoring force decreases gradually from the anchor head to the anchor tail. The anchoring force of each part of the anchor shaft increases with the anchoring time passed, but the increase magnitudes of the anchoring force at the same time are different. For instance, at the initial phase of the loading, the increase magnitudes of the anchoring force is larger. Take the anchoring force at the anchor head for example; the increase magnitudes of the anchoring force during excavation procedure are 98.18%, 39.69%, 14.75% and 0%.

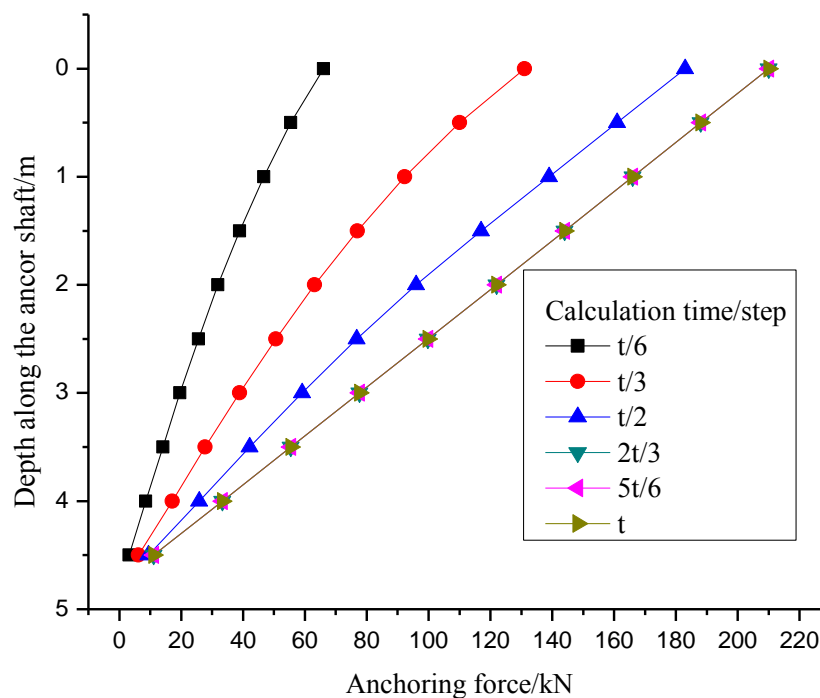


Figure 12: Axial stress transferring procedure of anchor

CONCLUSIONS

Numerical solutions for the following aspects are done: distribution of anchor axial stress, response of the soil, the effect of the surrounding stress to the limit anchoring force, and the effect of the anchor length to the limit anchoring force. Results show that, the axial stress of anchor reduces along shaft; During the loading procedure, the failure propagates rapidly along anchor shaft, and finally leads to the whole failure of anchor; The soil mass tends to be pulled out by anchor by the friction force of interface between anchor and soil mass; The increase of surrounding stress can lead to the increase of cohesion of the interface between anchor and surrounding soil mass, but with a limit magnitude.

ACKNOWLEDGMENT

The author wishes to acknowledge the support from Henan Province foundation and forefront technology research project (102300410140) for this paper.

REFERENCES

1. Zhao, Y.M. and Yang, M.J., (2011) "Pull-out behavior of an imperfectly bonded anchor system," *International Journal of Rock Mechanics & Mining Sciences*, 48, 469-475.
2. Jeon, S.S., (2012) "Pullout tests and slope stability analyses of nailing systems comprising single and multi rebars with grouted cement," *J. Cent. South Univ.*, 19, 262-272.
3. Yang, S.T., Wu, Z.M., Hu, X.Z., Zheng, J.J., (2008) "Theoretical analysis on pullout of anchor from anchor-mortar-concrete anchorage system," *Eng. Fract. Mech.*, 75, 961-985.
4. Wu, Z.M., Yang, S.T., Hu, X.Z., Zheng, J.J., (2007) "Analytical method for pullout of anchor from anchor-mortar-concrete anchorage system due to shear failure of mortar," *J. Eng. Mech.*, 133, 1352-1369.
5. Delhomme, F. and Debicki, G., (2010) "Numerical modeling of anchor bolts under pullout and relaxation tests," *Constr. Build. Mater.*, 24, 1232-1238.
6. Milligan, G.W.E. and Tei, K., (1998) "The pullout resistance of model soil nails," *Soils. Found.*, 38, 179-190.
7. Cai, F. and Ugai, K., (2003) "Reinforcing mechanism of anchors in slopes: a numerical comparison of results of LEM and FEM," *Int. J. Numer. Anal. Meth. Geomech.*, 27, 549-564.
8. Guo, R., and Thompson, P., (2002) "Influences of changes in mechanical properties of an overcored sample on the far-field stress calculation," *International Journal of Rock Mechanics & Mining Sciences*, 39, 1153-1166.
9. Gurung, N., (2001) "1-D analytical solution for extensible and inextensible soil/ rock reinforcement in pull-out tests," *Geotextiles and Geomembranes*, 19, 195-212.
10. Li, C. and Stillborg, B., (1999) "Analytical models for rock bolts," *Int. J. Rock Mech. Sci. and Geomech. Abstr.*, 36, 1013-1029.
11. Kaiser, P. K., (1992) "Effect of the stress change on the bond strength of fully grouted cables," *International Journal of Rock Mechanics and Mining Sciences & Geomechanical Abstracts*, 29, 293-306.
12. Huang, J. and Han, J., (2009) "3D coupled mechanical and hydraulic modeling of a geosynthetic-reinforced deep mixed column-supported embankment," *Geotextiles and Geomembranes*, 27, 272-280.
13. Gao, F.Q. and Kang, H.P., (2008) "Effect of pre-tensioned rock bolts on stress redistribution around a roadway-insight from numerical modeling," *Journal of China University of Mining and Technology*, 18, 509-515.

14. Cai, M., (2008) "Influence of stress path on tunnel excavation response – Numerical tool selection and modeling strategy," *Tunnelling and Underground Space Technology*, 23, 618-628.
15. Ghazavi, M., and Lavasan, A.A., (2008) "Interference effect of shallow foundations constructed on sand reinforced with geosynthetics," *Geotextiles and Geomembranes*, 26, 404-415.
16. Itasca Consulting Group., (2002) "User's Guide," Minnesota: itasca consulting group.

